

# RESISTIVITY-STRAIN ANALYSIS OF GRAPHENE-BASED INK COATED FABRICS FOR WEARABLE ELECTRONICS.

M. Simard-Normandin<sup>1</sup>, Q.-B. Ho<sup>2</sup>, R. Rahman<sup>1</sup>, S. Ferguson<sup>1</sup> and K. Manga<sup>2</sup>

1. MuAnalysis Inc.

Ottawa, ON, Canada

2. Grafoid Inc.

Kingston, ON, Canada

martine@muanalysis.com

kmanga@grafoid.com

## ABSTRACT

In this study, we have developed a method to prepare highly stable and conducting graphene-based ink to coat different types of fabrics, both woven and non-woven, and measured the change in resistivity as a function of stress and cyclic strain. The study shows promising results towards the application of conductive ink directly to fabric for wearable sensors.

Keywords: Graphene, wearable electronics, resistivity-strain, conductive ink, sensors.

## INTRODUCTION

Wearable electronic devices are gaining popularity. The trend is moving away from bracelet and watch-like devices to integrated sensors imbedded in clothing fabrics. [1-3] The benefits to health care of the development of such a variety of sensors are incommensurable. In terms of sensitivity and selectivity, sensors based on nanoscale properties have proved their superiority as compared to macroscale sensors. [4] These attractive features are contributed by the higher surface to volume ratio and larger active area of the nanoscale materials. Apart from that, the advantage of their smaller size facilitates easier integration into other material substrates, such as, polymer or other fabrics. [5] Among the nanostructural materials, the low resistivity of graphene and its extreme thinness make it an exciting candidate for the coating of various textiles to carry signals out to processing devices [6]. As well, small changes of resistivity as function of motion can be used to monitor respiration or other physiological factors. Unlike the resistive metal-oxide sensors, that comprise a significant part in the present market and require high temperature processing leading to higher power consumption and cost, [7] graphene based sensors can be processed at room temperature, thus reducing the processing cost and widening its application area. For this study, we considered application of graphene based ink on different types of clothing fabrics. However, the environment of clothing is harsh. The fabric is continuously bent and

stretched during the most mundane everyday activities. Different applications of wearable sensors will require different materials. Hence it is important to develop a conducting ink with good wettability and compatibility with all types of fabric materials. Graphene ink is particularly well suited for this application.

## EXPERIMENTAL METHODS

### Sample Preparation

The conducting graphene based ink used (Mesograf™ Ink, from Grafoid Inc.) was applied on to the fabric substrates through a spray nozzle under pressure to produce coatings with desired thickness. Additional air pressure was applied after each spray to improve the adhesion with the fabrics. The products were then cured at elevated temperatures to facilitate the evaporation of volatile chemicals and the formation of the coating network. The ink, as shown in Figure 1, demonstrated good dispersion and high stability over time.

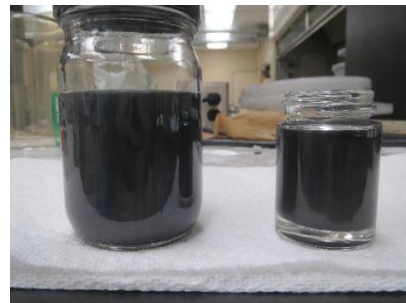
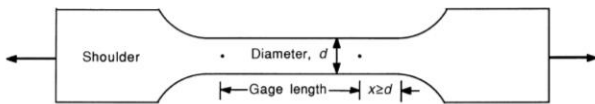


Figure 1. Mesograf Ink

The first group of tests was done using materials found around the lab: a piece of jeans, polyester from a lab coat and non-woven material from swabs. These were intended to develop the methodology, test the software and get a feel for the maximum resistivity for different types of fabrics. Rectangular strips 2-in wide and 6-in long were cut in preparation for coating.

These were found too wide of the tensile tester grips and they were cut longitudinally after coating into two 1-in wide strips. One strip was tested for resistivity-strain and one strip for resistivity-bend.

On the second group of tests, new material was purchased and cut according to the pattern shown in Figures 2 and 3. With a gage length of 3 inch, a diameter of 0.5 inch, and a shoulder with of 1 inch. We refer to them as dog-bone shaped samples in this paper. Long shoulders were left to allow wrapping of the material. The ink coating extended to the start of the shoulder to allow good contact between the electrodes and the coated fabric.



**Figure 2.** Geometry of fabrics from the second group.

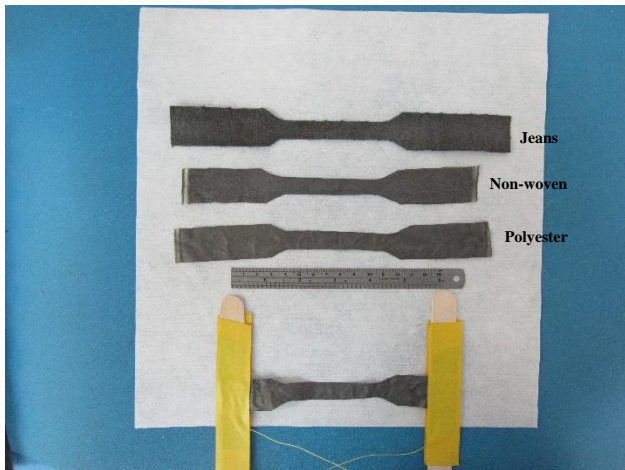


**Figure 3.** Different fabric samples after ink coating. One sample is shown with the contacts attached on both sides along with the insulated craft sticks to be held into the tensile tester grips.

## TEST AND CHARACTERIZATION

### Ink-Coating Stability Test

Ink coated jeans, polyester and non-woven fabrics were tested in water to see if there is any delamination of the coating. A strip of 1cm x 5cm of each fabric was clipped onto the inside of a beaker containing water and stirred on magnetic stirrers at 450 RPM for 16 hours, as shown in Figure 4. All the ink coated fabric samples showed good stability in water and no delamination observed even after sixteen hours of magnetic stirring (Figure 5).

The two groups of samples were coated at different times and the fabrics used, although of similar nature, were not identical. The initial sheet resistances are therefore different between the two batches (Table 1).

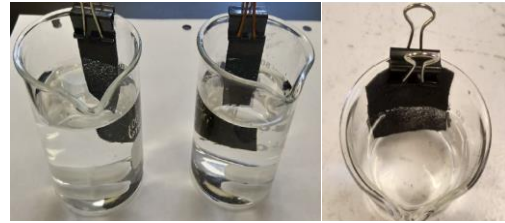
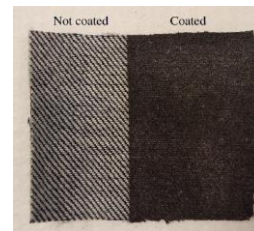


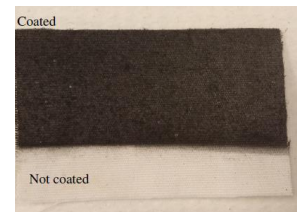
**Figure 4.** Samples for stability test.



(a)



(b)



(c)

**Figure 5.** From top to bottom: (a) jeans, (b) polyester, and (c) non-woven fabric samples without any delamination after 16 hours of magnetic stirring.

### Sensor Tensile Strength and Sensitivity Test

For tensile testing, mechanical strain was applied to the ink coated fabric samples using an Instron 4411 load frame (Figure 6). 5kN wedge grips with serrations in both faces were mounted in the Instron. A 5kN load cell was selected to accommodate the heavy wedge grips and any additional load generated by the fabric samples. The load and extension of the sample measured by the Instron were recorded by a PC using the Series IX software.



**Figure 6.** Instron 4411 tensile tester with a sample.

For electrical characterization, a Keithley 225 current source (Figure 7(a)) was used to inject  $100\mu\text{A}$  through the fabric sample. The voltage across the fabric sample was measured with a Keithley 2000 digital multimeter (DMM) (Figure 7(b)). The Instron also provided an analog voltage output linearly correlated to the instantaneous load cell reading. This voltage was measured by a second DMM and was used for synchronization of the resistivity to the extension. The maximum voltage of +10V corresponds to the full scale of the load cell used (5kN). The voltages corresponding to the fabric resistance and load cell output were continually logged by a separate computer.

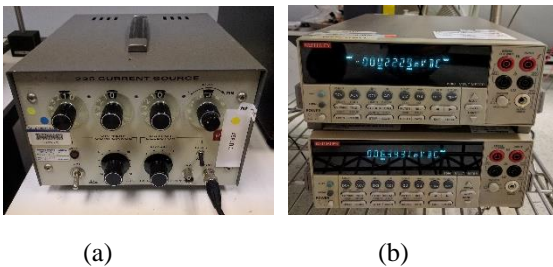


**Figure 7.** (a) Keithley 225 current source to provide current flow through the samples (b) Keithley 2000 digital multimeters to read the resistivity and track the load for synchronization to the Instron data.

To attach the sample fabrics to the tensile tester grips and prevent the slipping of the fabrics during the strain application, two pieces of large wooden craft sticks were used at the sample ends being taped to them. The sample ends were wrapped around the craft sticks along with the copper wire contacts for electrical measurements, as shown in Figure 8. When clamped in the Instron grips this arrangement prevented any slipping and clearly define the active or gage length. The two wooden sticks, one on either side, also prevented shorting between the fabric and the grips. The smooth surfaces of the craft sticks helped to prevent damage at the sample ends caused by the strain and the serrated grips.

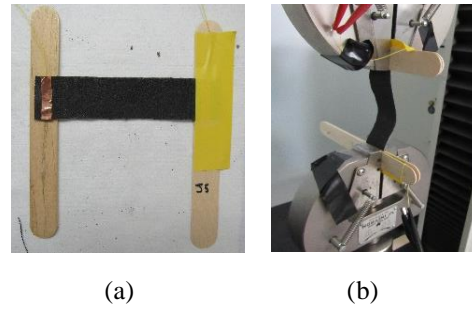


**Figure 8.** (a) A fabric sample with copper wire and copper tape contacts along with craft sticks attached on both sides (b) fabric placed in between the two grips.

## RESULTS AND DISCUSSION

### Tensile Strength Analysis

For the tensile strength test, a continuously increasing strain was applied in the longitudinal direction of the samples. An extension rate of 3mm/min was programmed into the Instron. Data was logged at a rate of 5pts/s. Resistance across the samples were simultaneously recorded during this test from the digital multimeter. The test was continued just past the initial break point. A tear in the fabric initiated at one side and propagated through the sample as extension. At the end of a successful test, approximately 9/10th of the sample width had ripped. Due to the destructive nature of the tensile strength test, multiple fabric samples having the same dimension were prepared to perform the cyclic strain tests later, thus preventing any damage or deformation of the fabric incurred during one test from altering the results of a subsequent test. For the dog-bone samples, only a limited number of samples were available, therefore, for a given fabric, the cyclic tests were performed first and the strength test last, all on one sample. This was possible because the overall resistivity of the samples was not affected by the cyclic tests.

The results of the tensile strength tests for different fabric samples are shown in Figures 9-14. The first three figures (9-11) show the stress-strain characteristics of the rectangular samples, whereas the following three figures (12-14) are obtained for the dog-bone shaped ones. The polyester samples showed more slippery nature than the jeans or non-woven ones, and were difficult to be held in the grips during the strain application. For the jeans samples, as shown in the Figures 9 and 12, the ultimate tensile strength was reached at a strain of 15.5% for the rectangular sample, whereas for the dog-bone shaped sample it was obtained at 20.53% of strain. Thus, the strain for the ultimate strength was increased significantly by changing the shape only, while keeping the gage length same. A similar effect was observed for the other two fabrics. For the polyester samples, while the ultimate tensile strength was achieved at a strain of 14.2% for the rectangular sample, it did not reach to that point even at the strain of 25% in case of the dog-bone shaped sample. For the non-woven samples, also we can find a similar

trend as we compare the Figures 11 and 14. The enhancement in the strain range for the ultimate strength can be attributed to the shoulder to gage geometry of the dog-bone shape samples. This geometry possibly has helped to distribute the load more uniformly during the strain application than the rectangular one. Therefore, the sensor geometry can play a critical role to determine the usable range of strain, and the sensor life as well.

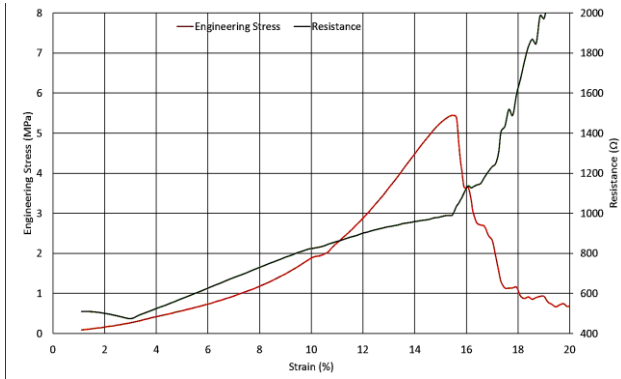


**Figure 9:** Jeans rectangular sample- Ultimate tensile strength was evaluated as approximately 5.5 MPa at a strain of 15.5%.

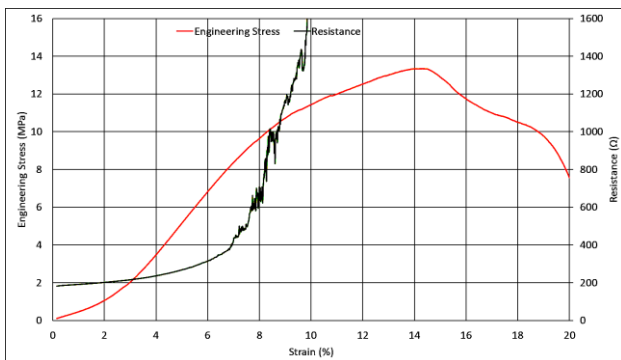


**Figure 10:** Polyester rectangular sample- Ultimate tensile strength was evaluated as approximately 13.1 MPa at a strain of 14.2%.

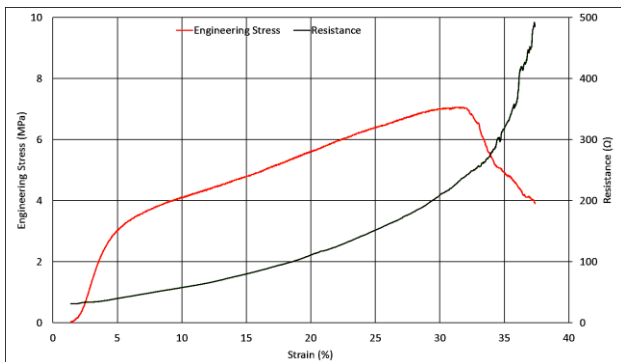


**Figure 11:** Non-woven rectangular sample- Ultimate tensile strength was evaluated as approximately 7.2 MPa at a strain of 32%.

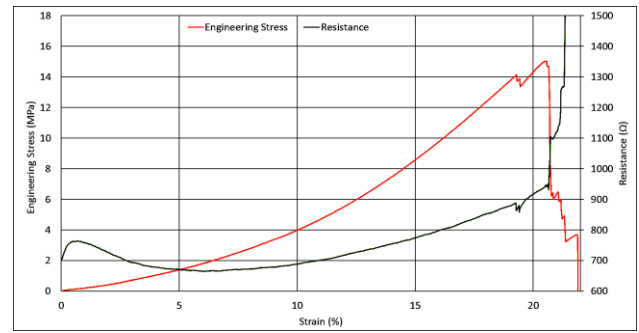


**Figure 12:** Jeans dog-bone shaped sample- Ultimate tensile strength was evaluated as approximately 15.03 MPa at a strain of 20.53%.

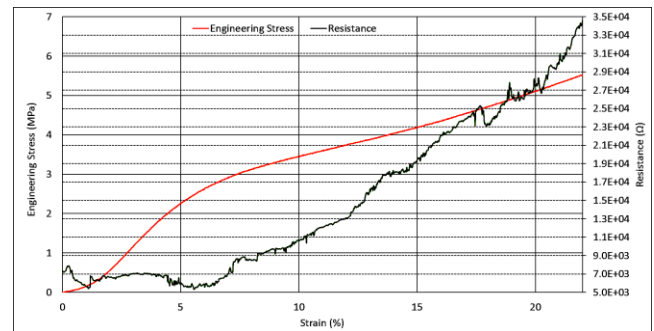


**Figure 13:** Polyester dog-bone shaped sample- Ultimate tensile strength was beyond the range of the applied strain.

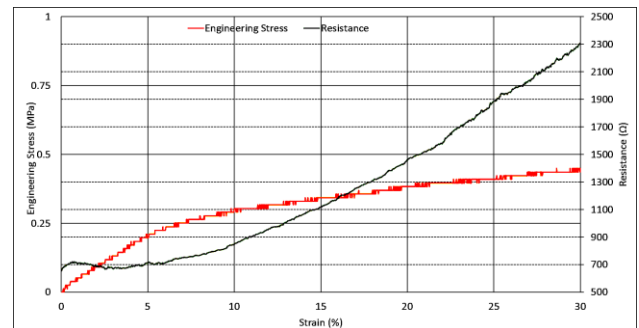


**Figure 14:** Non-woven dog-bone shaped sample- Ultimate tensile strength was beyond the range of the applied strain.

It was noted that, for the non-woven fabric samples, the tensile strength was noticeably less in comparison with woven fabrics, but its peak strength occurred at a much higher strain value. Different design windows are applicable for different types of strain sensors, depending on whether the sensor is meant for monitoring large-scale motions, such as knee bending or arm bending, or if it is for measuring small scale motions, such as blood pulse or respiration. The frequency of the motion is another parameter to consider as it influences the longevity and performance of the sensor materials. Depending on the sensing application, a trade-off will be necessary between

the tensile strength and strain range while designing the sensor geometry.

### Durability and Longevity Analysis

Durability of the strain sensors is one of the most important criterion to ensure their long-time application. Since these sensors are likely to encounter repeated loading-unloading of stress during everyday use, whether applied for large scale motion sensing or small-scale motion sensing, endurance and repeatability over multiple time cycles must be tested to confirm the consistency in their performance over time. We performed cyclic tests on the ink coated samples for at least 20 cycles of strain-relaxation. For each type of fabrics, the maximum strain was varied in between 1% and 3%. The percentile change in the resistance along with the strain was measured over repeated time cycles. Figures 15-20 show the results obtained for different fabric samples of the rectangular shapes.

All the rectangular samples showed consistent change in the resistance values during the strain and relaxation cycles, both for 1% and 3% cyclic strain applications. Although during the initial few cycles the resistance values were observed to be slightly off from resistance values during the later majority number of cycles, it can be considered as the transient phase right after the sensor starts experiencing the strain cycles. A possible explanation is a variation of the contact resistance as the test progresses. All the samples showed two local maxima for each cycle of strain, except the polyester sample that showed only one peak for each cycle during 1% cyclic strain tests. The multiple peaks can occur due to the re-orientation between the nanoparticles while the fabric substrate gets stretched, leading to the change in the inter-particle distance and the overall sample resistance. The consistency of the resistance change pattern even after the large number of cycles indicates good repeatability of our ink based sensors.

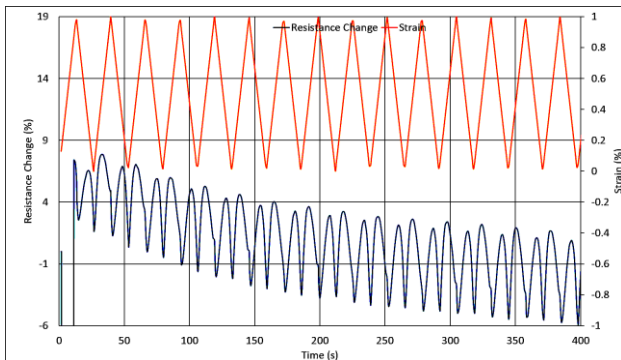


**Figure 15.** Jeans rectangular sample with maximum strain of 1%. Two resistance maxima observed per strain cycle. Amplitude of 7%. Local minimum at strain maximum.

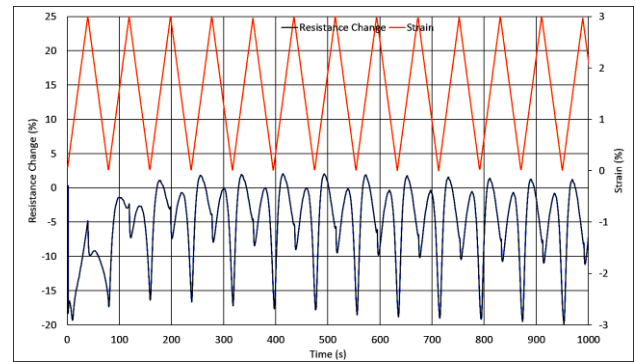


**Figure 16.** Jeans rectangular sample with maximum strain of 3%. Two resistance maxima are observed per strain cycle. Amplitude of 21%. Local minimum at strain maximum.

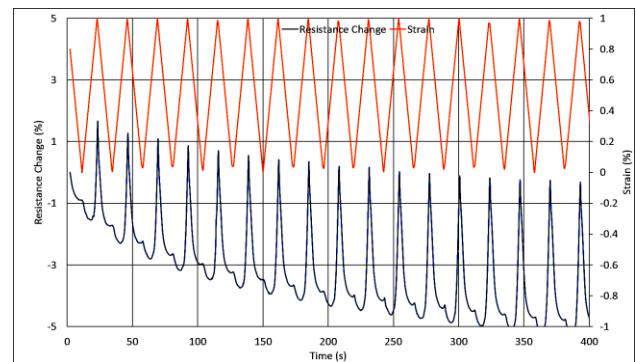


**Figure 17.** Polyester rectangular sample with maximum strain of 1%. Single spike observed per strain cycle. Amplitude of 5%. Resistance maximum coincides with strain maximum.

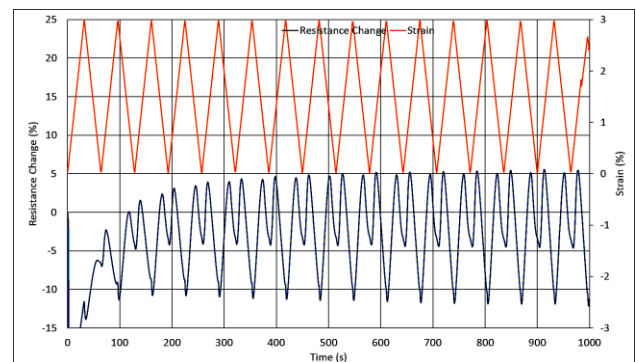


**Figure 18.** Polyester rectangular sample with maximum strain of 3%. Two resistance maxima per strain cycle. Amplitude of 17%. Local minimum at strain maximum.

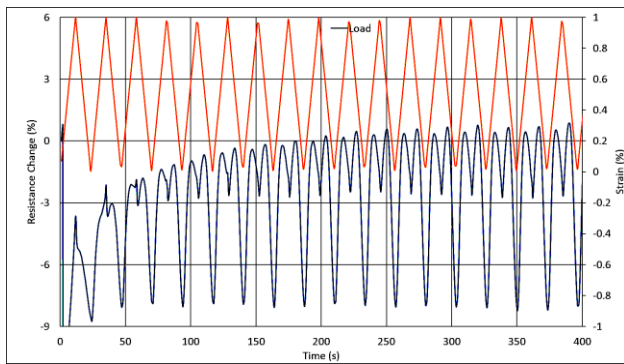


**Figure 19.** Non-woven rectangular sample with maximum strain of 1%. Two resistance maxima observed per strain cycle. Amplitude of 9%. Local minimum at strain maximum.

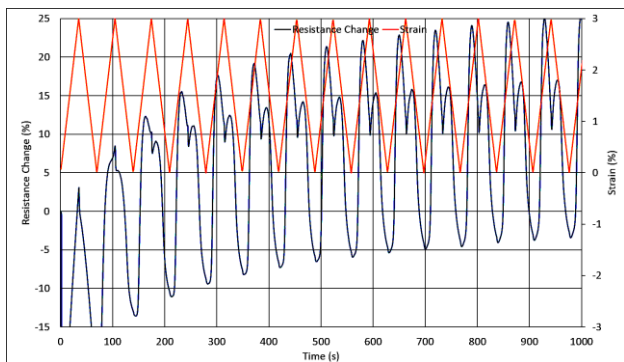


**Figure 20.** Non-woven rectangular sample with maximum strain of 3%. Two resistance maxima observed per strain cycle. Amplitude of 28%. Local minimum at strain maximum.

Similar cyclic strain tests (1% and 3%) were performed on the dog-bone shaped samples. The results for these samples are shown in the Figures 21-25. Here also we observed the similar consistency in the resistance change pattern with the strain-relaxation cycles, as seen for the rectangular samples. For the dog-bone shaped jeans samples the amplitude of the change in the resistance was either less than or comparable to that of the rectangular ones. For the non-woven samples, the resistance change amplitude was noticeably lower for the dog-bone shaped samples. This can be attributed to the improved load-transfer mechanism of the latter samples. Finally, for the polyester samples, we observed very high amplitude in the resistance change, and irregular spike patterns in between two cycles. This occurred because, for the same coating, different fabric substrates have different surface energy, which causes variation in the adherence of the coated liquid onto the substrate surface. Due to the comparative lower adherence, the uniformity of the graphene ink coating was more affected for this non-woven fabric during the applied strain, than the other two woven types of fabric. The inter-particle connectivity was deteriorated with aging and applied strain leading to lower conductivity. Since the 1% cyclic strain already caused

the loss of physical connection in the inter-nanoparticle network, we skipped the 3% cyclic strain test for the polyester samples.

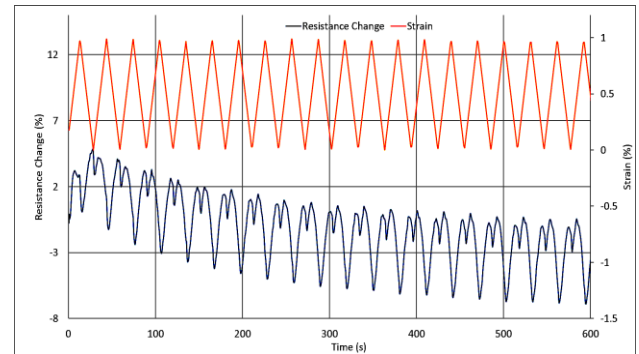


**Figure 21.** Jeans dog-bone shaped sample with maximum strain of 1%. Two resistance maxima observed per strain cycle. Amplitude of 6.5%. Local minimum at strain maximum.

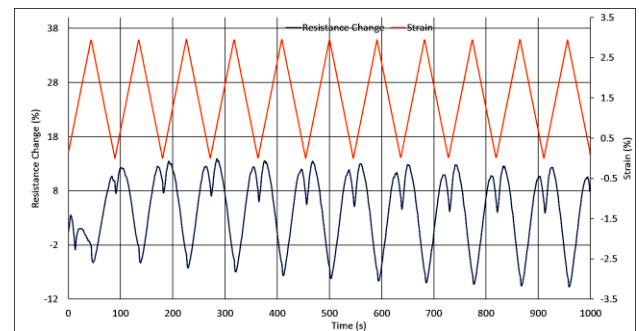


**Figure 22.** Jeans dog-bone shaped sample with maximum strain of 3%. Two resistance maxima observed per strain cycle. Amplitude of 22%. Local minimum at strain maximum.

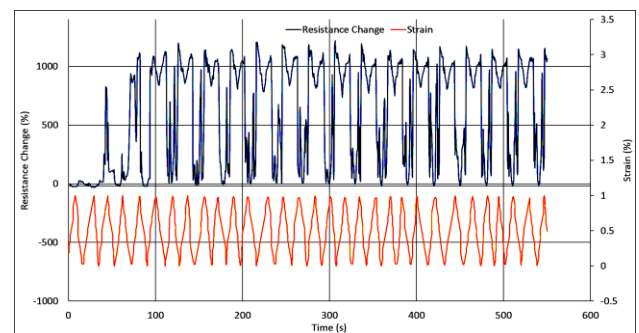


**Figure 23.** Polyester dog-bone shaped sample with maximum strain of 1%. Two resistance maxima observed per strain cycle. Amplitude of 1200%. Irregular spikes were observed in between two consequent cycles of resistance change due to the delaminated coating flakes formed during the sample stretching.

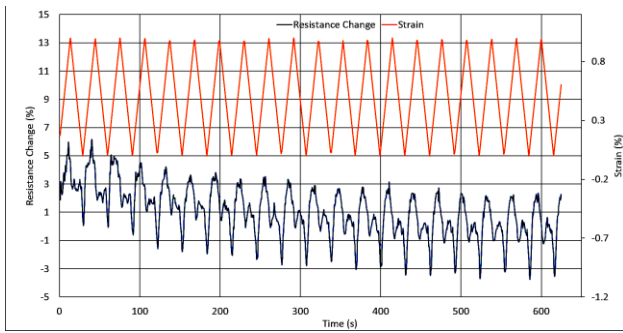


**Figure 24.** Non-woven dog-bone shaped sample with maximum strain of 1%. Two resistance maxima observed per strain cycle. Amplitude of 6%. Local minimum at strain maximum.

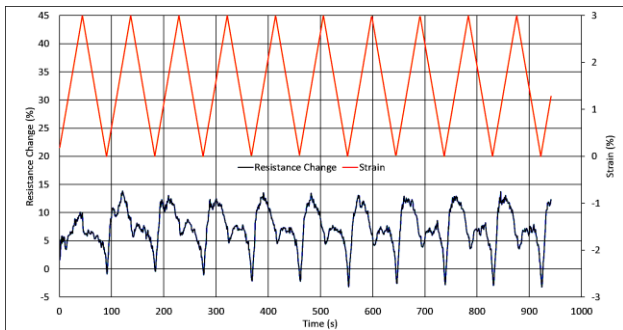


**Figure 25.** Non-woven dog-bone shaped sample with maximum strain of 3%. Two resistance maxima observed per strain cycle. Amplitude of 16%. Local minimum at strain maximum.

### Strain sensitivity analysis

The sensitivity of the ink coated sensors based on different fabrics was measured in terms of gauge factor. The gauge factor is the ratio of relative change in electrical resistance  $R$ , to the mechanical strain  $\epsilon$ .

$$GF = (\Delta R / R) / \epsilon$$

The applied strain was gradually increased to a maximum of 30%. Figure 26 shows the percentile change in the resistance and gauge factor for continuous strain application for rectangular jeans and Figure 27 for the rectangular non-woven samples. For both the fabrics, the gauge factor showed non-linear behavior. Non-woven fabric samples showed higher gauge factor than the jeans samples across all strain values. For the dog-bone shaped jeans and non-woven samples (Figures 28-29), again the non-woven samples showed a bit higher gauge factor than the jeans, not a significant difference though. In both cases, we observed a linear increase in the gauge factor within the range of 5-20% strain, and non-linear behavior at lower strain range. The polyester dog-bone shaped sample demonstrated delamination of the ink coating with increasing strain and became non-conductive (Figure 30). The rectangular polyester sample slipped out of the grips and yielded no useable results. This prompted the change

to the dog-bone geometry for the second set of measurements.

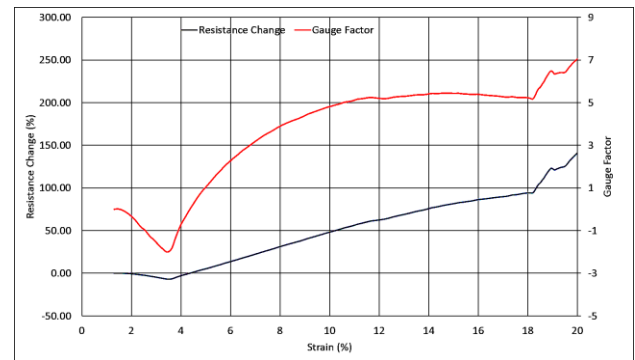


**Figure 26.** Jeans rectangular sample- Gauge factor and resistance change for strain of 20%.

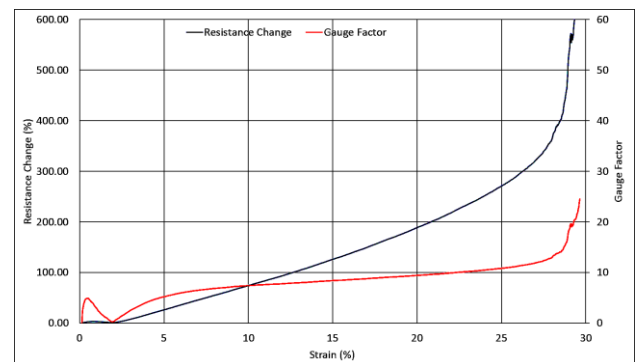


**Figure 27.** Non-woven rectangular sample- Gauge factor and resistance change for strain of 30%.

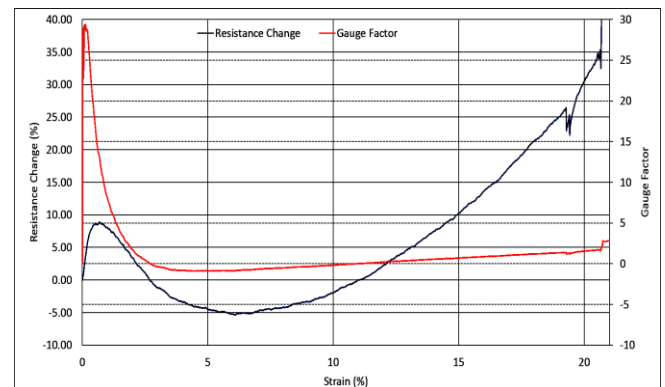


**Figure 28.** Jeans dog-bone shaped sample - Gauge factor and resistance change for strain of 20%.

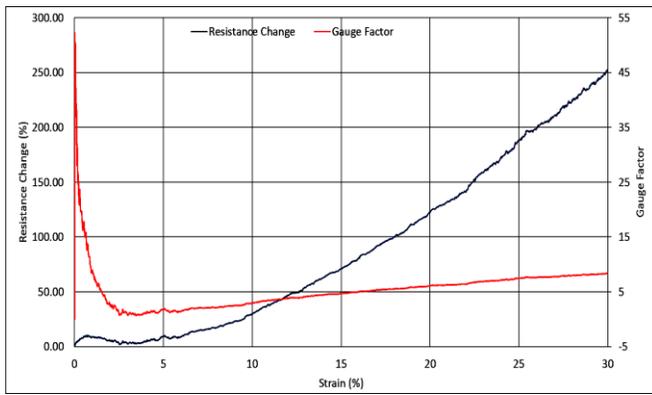


**Figure 29.** Non-woven dog-bone shaped sample - Gauge factor and resistance change for strain of 30%.

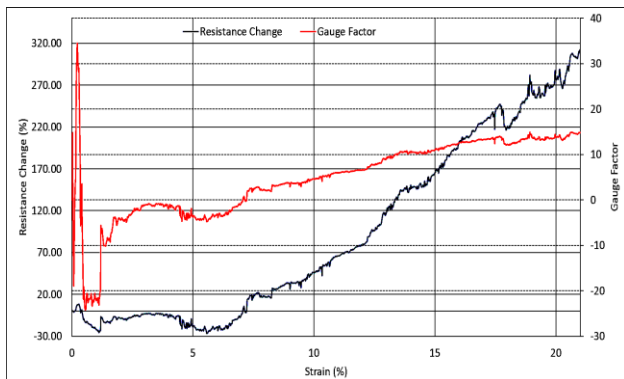


**Figure 30.** Polyester dog-bone shaped sample - Gauge factor and resistance change for strain of 20%.

**Table 1:** Summary of results

	Jeans		Polyester		Non-woven	
	Rectangular	Dog-bone shape	Rectangular	Dog-bone shape	Rectangular	Dog-bone shape
Ultimate Tensile Strength, UTS (MPa)	5.5	15.03	13.1	-	7.2	-
Strain at UTS (%)	15.5	20.53	14.2	>25	32	>30
Sheet Resistance, ( $\Omega$ /square)	69.2	116.2	20.9	71.1	64.1	90.4
Maximum Resistance change (%) at 1% cyclic strain	7	6.5	5	1200	9	6
Maximum Resistance change (%) at 3% cyclic strain	21	22	17	-	28	16
Gauge factors at low strain (1%, 3%)	7, 7	6.5, 7.3	5, 5.7	-	9, 9.3	6, 5.3
Gauge factor at high strain (20%)	7	1.54	-	13.6	9.43	6.15

## DISCUSSION

Our results are summarized in Table 1. The variation of sheet resistance between samples of similar fabrics but different shapes is possibly due to the variation in the experimental parameters executed at two different times. In all cases our sheet resistance results keep within the range of graphene resistivity [8]. The gauge factors at low strain showed reasonable consistency for all the fabric types. However, for higher strain range, the non-woven fabric samples show nearly identical sensitivity, whereas the woven samples show variations. The possible reason can be the difference in the surface topology. Non-woven samples used in this study are flat and continuous. The interlaced texture of the woven samples, even of similar fabrics, can vary significantly when they come from different sources. The yarns can separate at different loads and break the continuity of the coated ink layer.

Our graphene based ink coated non-woven fabric shows consistency in gauge factor with previously reported results using reduced graphene oxide (rGO) [9] coated non-woven fabric, even higher for some samples. These results show the first step of our investigation towards finding the effect of different parameters, including the fabric type, sample shapes, weaving variations and direction, on the strain sensitivity of graphene based wearable sensors.

## CONCLUSION

A graphene-based ink was coated on different fabric materials (jeans, non-woven and polyester) using a wet chemistry method. The electro-mechanical properties of the coated samples were characterized from the change in their resistivity with the application of linear strain. The fabric samples show different sensitivity based on adhesion and interactions with the ink. The geometry of the sensor is revealed to play a critical role in determining the active strain range, and works as a key parameter in determining the design window of the sensors. The ink also showed good longevity and durability, though the strain repeatability range varied in different fabrics due to different surface energy.

## REFERENCES

1. T. Yamada, Y. Hayamizu, Y. Yamamoto, Y. Yomogida, A. Izadi-Najafabadi, D. N. Futaba and K. Hata, *Nat. Nanotechnol.*, 2011, 6, 296–301.
2. M. Segev-Bar and H. Haick, *ACS Nano*, 2013, 7, 8366–8378.
3. D. Son, J. Lee, S. Qiao, R. Ghaffari, J. Kim, J. E. Lee, C. Song, S. J. Kim, D. J. Lee, S. W. Jun, S. Yang, M. Park, J. Shin, K. Do, M. Lee, K. Kang, C. S. Hwang, N. Lu, T. Hyeon and D.-H. Kim, *Nat. Nanotechnol.*, 2014, 9, 397–404.
4. H. Yoon, J. Xie, J. K. Abraham, V. K. Varadan, and P. B. Ruffin, *Smart Mater. Struct.*, 2006, 15, S14-S20.
5. R. Rahman, S. Soltanian, and P. Servati, *IEEE Sensors Journal*, 2016, 16, 77-87.
6. Y. Wang, L. Wang, T. Yang, X. Li, X. Zang, M. Zhu, K. Wang, D. Wu and H. Zhu, *Adv. Funct. Mater.* 2014, 24, 4666–4670.
7. R. Rahman, and P. Servati, *IEEE Transaction on Nanotechnology*, 2015, 14, 118-129.
8. S. Bae, H. Kim, Y. Lee, X. Xu, J. Park, Y. Zheng, J. Balakrishnan, T. Lei, H. Kim, Y. Song, Y. Kim, K. Kim, B. Özyilmaz, J. Ahn, B. Hong, and S. Iijima, *Nature Nanotechnology*, 2010, 5, 574–578.
9. D. Du, P. Li, J. Ouyang *J. Mater. Chem. C*, 2016, 4, 3224.